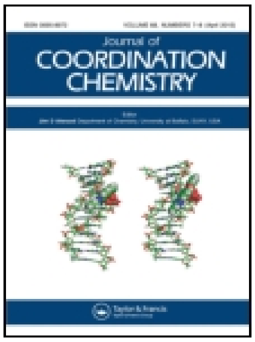

Journal of Coordination Chemistry

ISSN: 0095-8972 (Print) 1029-0389 (Online) Journal homepage: http://www.tandfonline.com/loi/gcoo20

Tin-derivative sandwich-type polyoxometalates supported on Nd-doped TiO_2 nanoparticles as efficient and reusable catalysts in the oxidation of sulfides and alcohols

Liela Bahrami, Roushan Khoshnavazi & Amin Rostami

Journal of Coordination Chemistry, 2015
Vol. 68, No. 23, 4143–4158, http://dx.doi.org/10.1080/00958972.2015.1095889

Tin-derivative sandwich-type polyoxometalates supported on Nd-doped TiO_2 nanoparticles as efficient and reusable catalysts in the oxidation of sulfides and alcohols

LIELA BAHRAMI, ROUSHAN KHOSHNAVAZI* and AMIN ROSTAMI

Department of Chemistry, University of Kurdistan, Sanandaj, Iran

(*Received 4 April 2015; accepted 2 September 2015*)

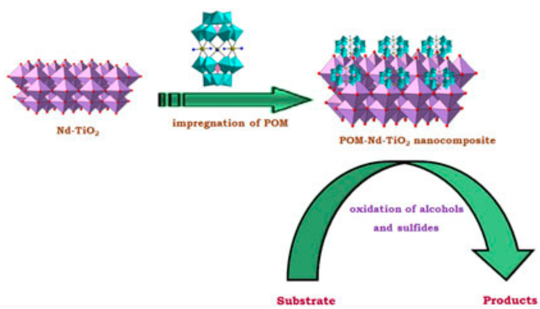

New nanocomposites, including different loading levels of sandwich-type polyoxometalates $[(HOSn^{IV}OH)_3(XW_9O_{34})_2]^{n-}$ (X = As (**1**), P (**2**) $n = 12$ and Si (**3**) $n = 14$) on Nd-doped TiO_2 nanoparticles were prepared by a simple impregnation method. The nanocomposites were characterized by X-ray diffraction (XRD), scanning electron microscopy, transmission electron microscopy, Fourier transform infrared (FTIR), and energy-dispersive X-ray spectroscopy. Compounds **1**–**3** were successfully loaded on Nd-doped crystallized anatase-phase TiO_2 nanoparticles of 20–25 nm. Catalytic activities of nanocomposites were examined by carrying out the oxidation of sulfides and alcohols with H_2O_2. Simple synthesis method, reusability, and low amounts of the heterogeneous catalysts with a slight excess of H_2O_2 and mild reaction conditions make these oxidation reactions an environmentally benign chemical process.

Keywords: Tin-derivative sandwich-type polyoxometalates; Nd-doped titanium dioxide; Nanocomposite; Heterogeneous catalyst

1. Introduction

Polyoxometalates (POMs) are composed of negatively charged inorganic metal-oxygen-building blocks and cations. These compounds can self-assemble into 3-D

*Corresponding author. Email: r.khoshnavazi@uok.ac.ir

structures with special electronic structures at multilevel length scales [1, 2]. The diversity in composition and structure of POMs make them attractive materials in many fields, including their use as catalysts in oxidation and acid-assisted reactions [3]. POMs exhibit catalytic activity in the oxidation of olefins to epoxides, oxidative dehydrogenation of alkanes or isomerization reactions, which has attracted attention in both homogeneous and heterogeneous catalysis [4–7]. Despite some advantages, there are some drawbacks concerning catalysis with POMs-based systems; they are nonporous solids with a small surface area (<10 m^2/g) and have high solubility in polar solvents. Therefore, in a homogeneous catalytic reaction, the isolation of the products and reuse of the catalyst become difficult. To overcome these limitations, POMs have been supported on inert or weakly acidic materials with high surface area [8–10]. In recent years, numerous studies have focused on catalytic properties of Keggin and Dawson-type polyoxometalates. Sandwich-type polyoxometalates in which three or four metal ions are sandwiched between two Keggin or Dawson moieties, a well-known class of polyoxometalates, have been less studied. The catalytic properties of these compounds may be improved due to synergistic effect of metal ions and polyoxometalates. Many structural species of such polyoxometalates are known but attention has focused more on the transition-metal-substituted sandwich-type polyoxometalates. Neumann and coworkers used the sandwich-type transition metal-substituted polyoxometalate $K_{10}[(WZnRh^{III}{}_2)(ZnW_9O_{34})_2]$ for the epoxidation of alkenes [11]. Sandwich-type polyoxometalates of $Na_x[(WZnM^{II}{}_2(ZnW_9O_{34})_2]$ (M = Ru, Mn, Zn, Pd, Pt, Co, Fe, Rh) [12] were used as an effective catalyst for the selective oxidation of alcohols by aqueous hydrogen peroxide in a biphasic medium [13]. These and other transition-metal polyoxometalates have also been used for oxidative transformations with iodosobenzene [14], *N*-oxides [15], periodate [16], ozone [17], nitrous oxide [18], sulfoxides [19], molecular oxygen [20], and hydrogen peroxide [21, 22] as oxidants. Sandwich-type polyoxometalates of $K_{10}[(PW_9O_{34})_2M_4(H_2O)_2]$ (M^{II} = Co, Zn, Mn) for the oxidation of arenes and phenols [23], immobilized $\{(TBA)_7H_3[Co_4(H_2O)_2(PW_9O_{34})_2]\}$ into the 3-D porous metal-organic framework [24] as a recyclable catalyst for the oxidation of different substrates in solution and $Na_4K_5[K_3Cu_3(NO_3)(A\text{-}\alpha\text{-}PW_9O_{34})_2]$ for the epoxidation of alkenes [25] have been reported. Sandwich-type polyoxometalates containing main group metal ions were synthesized first by Pope in 1996. In this research, we investigate the catalytic properties of tin-containing sandwich-type polyoxometalates, $[(HOSn^{IV}OH)_3(XW_9O_{34})_2]^{n-}$. To the best of our knowledge, there is no report on the catalytic properties of these sandwich-type polyoxometalates. Tin-containing sandwich-type polyoxometalates are more hydrolytically stable than transition metal-substituted sandwich-type polyoxometalates in aqueous solution [26–28] and thus are more suitable for oxidation reactions. To overcome limitations of surface area, separation and recycling and, of course, to improve efficiency, sandwich-type polyoxometalates were supported on Nd-doped TiO_2 nanoparticles. A series of effective nanocomposites including different loading levels of sandwich-type polyoxometalates of $[(HOSn^{IV}OH)_3(XW_9O_{34})_2]^{n-}$ (X = As (**1**), P (**2**) $n = 12$ and Si (**3**) $n = 14$) (10–30%) on Nd-doped TiO_2 nanoparticles were prepared by simple impregnation method and were used as heterogeneous catalysts. The catalytic activities of the tin-containing sandwich-type polyoxometalates and the prepared nanocomposites were examined in reactions such as oxidation of alcohols and sulfides with H_2O_2.

2. Experimental

2.1. *Chemical and apparatus*

All reagents were commercially obtained and used without purification. Neodymium chloride hexahydrate ($NdCl_3{\cdot}6H_2O$), titanium(IV) isopropoxide (TTIP) and absolute ethanol were obtained from Merck. Potassium salts of $[(HOSn^{IV}OH)_3(XW_9O_{34})_2]^{n-}$ (X = As (**1**), P (**2**) $n = 12$ and Si (**3**) $n = 14$) were prepared according to the literature [26, 27]. The crystal structure of the synthesized nanocomposites were characterized by an X'PertPro Panalytical, Holland diffractometer in 40 kV and 30 mA with CuKα radiation ($\lambda = 1.5418$ Å). Infrared spectra were recorded on a Bruker Vector 22 FTIR using KBr pellets. The morphology of nanocomposites was revealed by a scanning electron microscope (FESEM-TESCAN MIRA3) and a transmission electron microscope (TEM, Zeiss – EM10C – 80KV). TEM images of the samples were prepared by dropping the ethanol dispersion on a lacey carbon-coated grid Cu Mesh 300. The elements in the nanocomposite were probed by energy-dispersive X-ray (EDX) spectroscopy accessory to the FESEM-TESCAN MIRA3 (SEM).

2.2. *Preparation of Nd-TiO$_2$ nano-sized*

Nd-TiO_2 nano-sized was synthesized using the reported procedure [29]. About 10 mL of $Ti\{OCH(CH_3)_2\}_4$ was added to 30 mL of EtOH at room temperature. Concentrated HCl was added to the mixture to obtain pH 1.5, and the solution was marked as **A**. $NdCl_3{\cdot}6H_2O$ (0.2 mmol, 0.07 g), the lanthanide precursor, was dissolved into the solution containing H_2O (2 mL) and EtOH (4 mL) and was marked as **B**. Then, solution **B** was added dropwise into the **A** solution in approximately 10 min. The resulting acidic mixture was stirred constantly for 12 h until the sol was obtained. The sol was maintained for 24 h until gel formation. The gel was dried at 373 K for 4 h and then calcinated at 823 K for 3 h. The lanthanide doping in the support is 1.0% [29].

2.3. *Preparations of catalyst nanocomposites (1a–3a)*

Nano Nd–TiO_2 (1 g) was dispersed in the separated water solution containing an appropriate amount (10, 20, and 30% w/w) of **1**–**3** POM precursors. The suspension was stirred continuously at room temperature. After continuously stirring for 24 h, the resulting products were dried in the oven at 373 K for 2 h. The final nine products were labeled **1a** (10, 20, and 30% w/w of **1**), **2a** (10, 20, and 30% w/w of **2**) and **3a** (10, 20, and 30% w/w of **3**).

2.4. *General procedure for oxidation of sulfides to sulfoxides*

2a (20%, 50 mg) was added to a mixture of sulfide (1 mmol) and 30% H_2O_2 (6–8 mmol) in CH_3CN (3 mL) and the mixture was stirred at room temperature for the time specified (table 1). Progress was monitored by TLC (EtOAc/*n*-hexane, 4/10). After completion of the reaction, the catalyst was separated from the product by centrifuge. The product was extracted with CH_2Cl_2 (3 × 5 mL) and the combined organic solutions washed with brine (10 mL) and dried over anhydrous Na_2SO_4. The solvent was removed under reduced pressure to give the corresponding pure sulfoxide in most cases.

Table 1. Optimization of the reaction conditions with respect to the effect of catalysts and solvents on the oxidation of methyl phenyl sulfide (1 mmol) using H_2O_2 (6 mmol) at room temperature.

Entry	Catalyst (mg)	Solvent	Time (min)	Sulfoxide (%)[a]	Sulfone (%)[a]
1	Catalyst-free	CH_3CN	2040	50	–
2	TiO_2	CH_3CN	2040	25	25
3	Nd–TiO_2	CH_3CN	2040	25	25
4	**1**	CH_3CN	720	Trace	–
5	**2**	CH_3CN	720	Trace	–
6	**3**	CH_3CN	720	Trace	–
7	Catalyst (**1a**) 20% (50)	CH_3CN	5	100	–
8	Catalyst (**2a**) 20% (50)	CH_3CN	10	–	100
9	Catalyst (**3a**) 20% (50)	CH_3CN	10	–	100
10	Catalyst (**1a**) 10% (100)	CH_3CN	12	100	
11	Catalyst (**2a**) 10% (100)	CH_3CN	20	–	100
12	Catalyst (**3a**) 10% (100)	CH_3CN	20	–	100
13	Catalyst (**1a**) 40% (50)	CH_3CN	120	30	–
14	**1a** 10% (100) Naked TiO_2	CH_3CN	25	100	–
15	Catalyst (**1a**) 20% (50)	H_2O	5	100	–
16	Catalyst (**2a**) 20% (50)	H_2O	5	100	–
17	Catalyst (**2a**) 20% (50)	H_2O	5	100	–

[a]Conversions determined by GC.

2.5. *General procedure for the oxidation of sulfides to sulfones*

Typically, **2a** (20%, 50 mg) was added to a mixture of sulfide (1 mmol) and 30% H_2O_2 (6–20 mmol) in H_2O (1.5 mL) and the mixture was stirred at room temperature for the time specified (table 2). Progress was monitored by TLC (EtOAc/*n*-hexane, 4/10). After completion of the reaction, the catalyst was separated from the product by centrifuge. The product was extracted with CH_2Cl_2 (3 × 5 mL) and the combined organic solutions washed with brine (10 mL) and dried over anhydrous Na_2SO_4. The solvent was removed under reduced pressure to give the corresponding pure sulfone in most cases.

2.6. *General procedure for oxidation of benzylic alcohols*

To a mixture of alcohol (1 mmol) and POMs-Nd-TiO_2 (40 mg) in H_2O (1 mL), 30% H_2O_2 (6–8 mmol) was added and the mixture was stirred at 80 °C for the time specified (table 3). Progress was monitored by TLC (EtOAc/*n*-hexane, 4/10). After completion of the reaction, the mixture was cooled to room temperature and the catalyst was separated from the product by centrifuge. The product was extracted with CH_2Cl_2 (3 × 5 mL) and the combined organic extractions washed with brine (10 mL) and dried over anhydrous Na_2SO_4. The solvent was removed under reduced pressure to give the corresponding pure carbonyl compound in most cases.

3. Results and discussion

3.1. *Preparation and characterization of POM-Nd-TiO_2 nanocomposites*

Various synthetic techniques have been developed to produce TiO_2 in different forms [30–37]. The sol–gel method with metal alkoxides as starting materials is widely used to obtain

Table 2. Selective oxidation of sulfides to sulfoxides or sulfones using H_2O_2 catalyzed by **2a.**

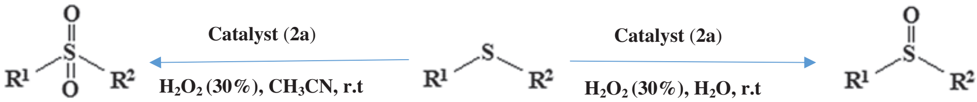

R^1, R^2= aryl, benzylic and alkyl

		Sulfoxide[a,b]		Sulfone[a,c]	
Entry	Substrate	Time (min)	Isolated yield (%)	Time (min)	Isolated yield (%)
1[d]	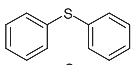	120	90	40	90
2	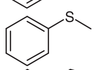	5	90	10	90
3	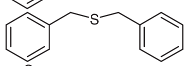	5	90	10	90
4	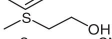	10	90	20	90
5	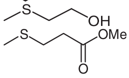	10	91	40	90
6	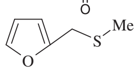	10	90	20	90

[a]All the products are known and were characterized by IR and ^1H NMR and by melting point comparison with those of authentic samples [47, 48].
[b]Reaction conditions: sulfide (1 mmol), 30% H_2O_2 (6 mmol), catalyst **2a** (50 mg), H_2O, r.t.
[c]Reaction conditions: sulfide (1 mmol), 30% H_2O_2 (8 mmol), catalyst **2a** (50 mg), CH_3CN, r.t.
[d]Reaction conditions: sulfide (1 mmol), 30% H_2O_2 (20 mmol), catalyst **2a** (50 mg), H_2O, r.t.

titanium oxide nanoparticles [38]. The sol–gel technique and impregnation method were used for the preparation of POM–Nd–TiO_2 nanocomposites. In this research, sandwich-type polyoxometalates of $[(HOSn^{IV}OH)_3(XW_9O_{34})_2]^{n-}$ (X = As (**1**), P (**2**) $n = 12$ and Si (**3**) $n = 14$) as potassium salt are placed by different loadings (10–30%) onto the Nd–TiO_2 nanoparticle by impregnation. Desired polyoxometalates are prepared from the oxidation of $[(Sn^{II})_3(XW_9O_{34})_2]^{n-}$ (X = As, P, Si) by bromine [27]. The tin(IV) derivatives consist of two A-type $XW_9O_{34}{}^{n-}$ anions linked by three tin(IV) cations into an assembly of virtual D_{3h} symmetry (figure 1). Each Sn has two terminal OH^- ligands due to high charge on the Sn^{IV} [39–41]. Consistent with the elemental analysis, acid/base titrations show that **1**, **2** and **3** have one acidic proton. The surface of Nd–TiO_2 particles is positively charged in acidic

Table 3. Optimization of the reaction conditions with respect to the effect of catalysts on the oxidation of benzyl alcohol (1 mmol) to benzaldehyde using H_2O_2 (6 mmol) in H_2O at 80 °C.

Entry	Catalyst 20% (40 mg)	Time (h)	Benzaldeyde (%)[a]
1	Catalyst-free	24	50
2	Nd–TiO_2	24	10
3	**1**	10	50
4	**2**	10	70
5	**3**	10	25
6	**1a**	4	90
7	**2a**	4	90
8	**3a**	5	90

[a]Conversions determined by GC.

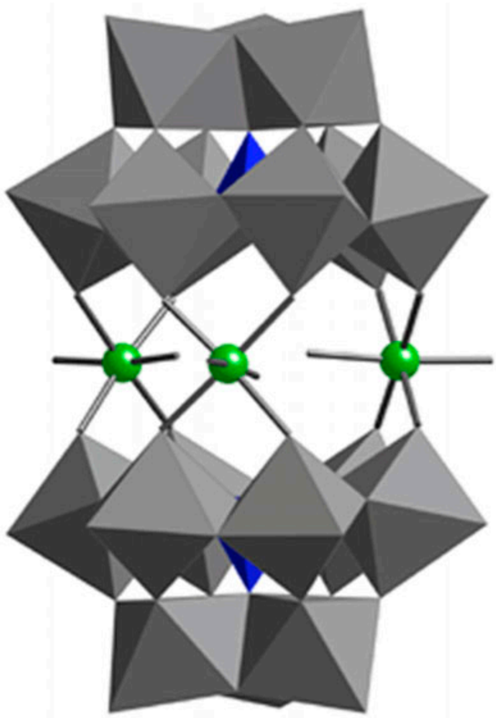

Figure 1. Polyhedral representation of $[(HOSn^{IV}OH)_3(XW_9O_{34})_2]^{n-}$. The polyhedra represent WO_6 and XO_4.

media, whereas the POMs are negatively charged, thus facilitating the adsorption of the POM species on the surface of TiO_2 particles by simple Coulombic interactions. The interaction of acidic hydrogen of **1**, **2,** and **3** may occur by an exchange reaction leading to the formation of water and the replacement of the surface hydroxyl anion by a polyoxometalate anion [42, 43]. Furthermore, Sn ions in the structures may have interaction with the surface of TiO_2 nanoparticles via their external OH groups. Therefore, by simple impregnation process, sandwich-type polyoxometalates strongly interact via oxygen atoms, through acidic hydrogen and also external OH groups of Sn ions with a surface of titania nanoparticles.

3.2. *Characterization of POM-Nd-TiO$_2$ nanocomposites*

3.2.1. FTIR analysis. The infrared spectra of POM–Nd–TiO_2 nanocomposites show characteristic absorptions of polyoxometalate units and Nd–TiO_2 nanoparticle. Figure 2 shows the FTIR spectra of Nd-TiO_2, **2** and its nanocomposites (**2a**) with 10–30% loadings as an example. The characteristic absorption peaks of **2** at 1087, 1024, 953, 899, 767, and 689 cm^{-1} correspond to $\nu_{as}(P–O_a)$, $\nu_{as}(W{=}O_d)$ and $\nu_{as}(W–O_{b,c}–W)$, respectively [27]. From figure 2(a), it can be seen that the IR spectrum of Nd–TiO_2 illustrates an intense, broad, indistinct region between 1100 and 400 cm^{-1}. The typical bands for absorption of P–O (1090 and 1020 cm^{-1}) and W–O (953 cm^{-1}) are clearly displayed in the nanocomposites spectra. The absorption peak intensity increases by increasing the amounts of loading

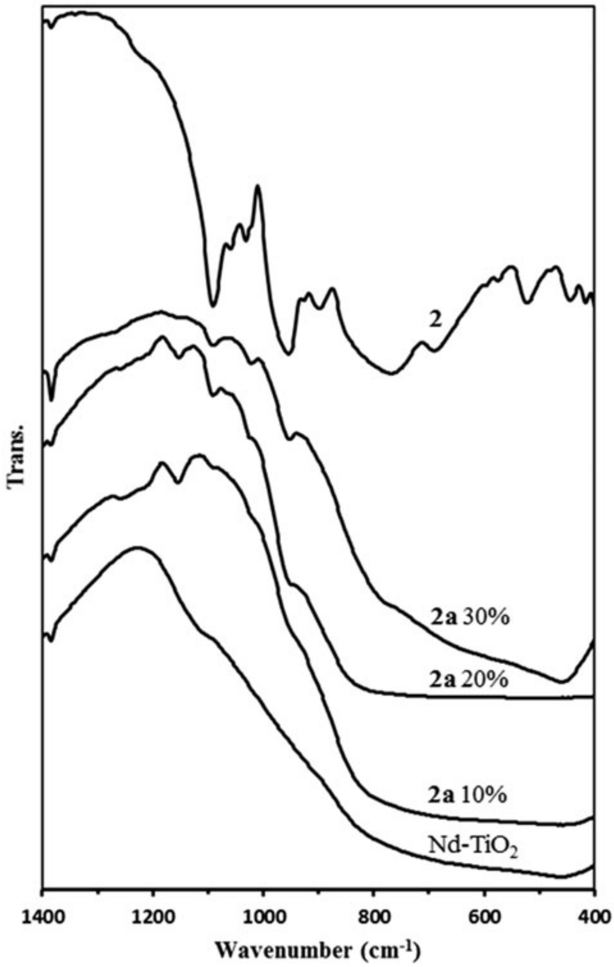

Figure 2. FTIR spectra of the prepared nanocomposites Nd-TiO_2, **2a** (10–30%) and $[(HOSn^{IV}OH)_3(PW_9O_{34})_2]^{12-}$.

polyoxometalate on the Nd–TiO_2. As a result, some characteristic peaks of POM unit in **2a** composites and other composites are overlapped in this area (see figure 2). FTIR spectra of other samples are given in the Supporting Information (figures S1 and S2). Attenuated total reflectance Fourier Transform IR spectroscopy (ATR FTIR) has been used for surface analysis of the nanocomposites. As expected, the appearance of POMs component on the surface of the prepared nanocomposites must be greater than that expected from the mass ratio. The ATR FTIR spectrum of **2a** shows strong peaks corresponding to **2**, evidence for loading the desired POM. The ATR FTIR spectrum of **2a** is given in the Supporting Information (figure S3).

3.2.2. X-ray diffraction analysis. Figure 3 shows the X-ray diffraction (XRD) testing results. XRD patterns of Nd-TiO_2 and pure TiO_2 are similar; both of them crystallized in

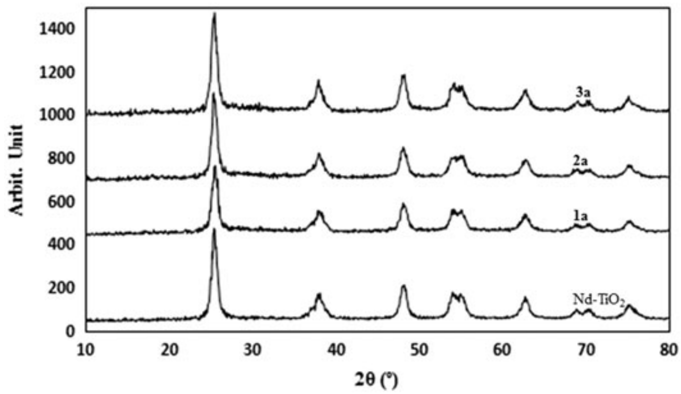

Figure 3. XRD patterns of Nd–TiO_2 and 20% POM loading of **1a**, **2a,** and **3a**.

the anatase structure with characteristic diffraction peaks of 2θ values located at 25.3°(101), 37.9°(004), 48.1°(200), 54.0°(105) and 62.7°(211) [44]. However, no characteristic peak of neodymium oxide is found, which implies that neodymium oxide content is very small and highly dispersed [45]. From figure 3 it can be seen that all the nanocomposites with 20% loading levels also have an anatase phase, and only anatase phase is present and no separate polyoxometalate-related phase is observed. These features probably result in the high dispersity of POM on Nd–TiO_2 nanoparticles [46]. The particle diameters calculated from the Debye–Scherrer formula are 20–50 nm.

3.2.3. SEM and TEM images. The SEM images **1a** (20%), **2a** (20%), and **3a** (20%) reveal that particles are regular spheres and less than 30 nm in diameter (figure 4), which is consistent with the XRD results. The TEM images of **1a** (20%) and **2a** (20%) are presented in figure 5, which reveal that most of the particles have a spherical shape. The average size of these nanoparticles is 20–30 nm which show a close agreement with the SEM images and the values calculated by XRD analysis.

3.2.4. EDX spectra. The composition of the nanocomposites was characterized by energy dispersive X-ray analysis (EDX). The EDX spectra confirm the expected elemental composition of nanocomposites. Figure 6 shows the EDX spectrum of **2a** (20%) which confirms its elemental composition (Nd, Ti, P, W, Sn and K). The EDX spectra of other samples are given in the Supporting Information (figures S4 and S5).

4. Catalytic application of POMs–Nd–TiO_2

4.1. *Catalytic application of POMs–Nd–TiO_2 in the oxidation of sulfides to sulfoxides and sulfones*

The chemoselective preparation of sulfoxides and sulfones is extremely important in organic chemistry. Organosulfur compounds, such as sulfoxides and sulfones, are valuable intermediates for the synthesis of fine chemicals and biologically active compounds [47].

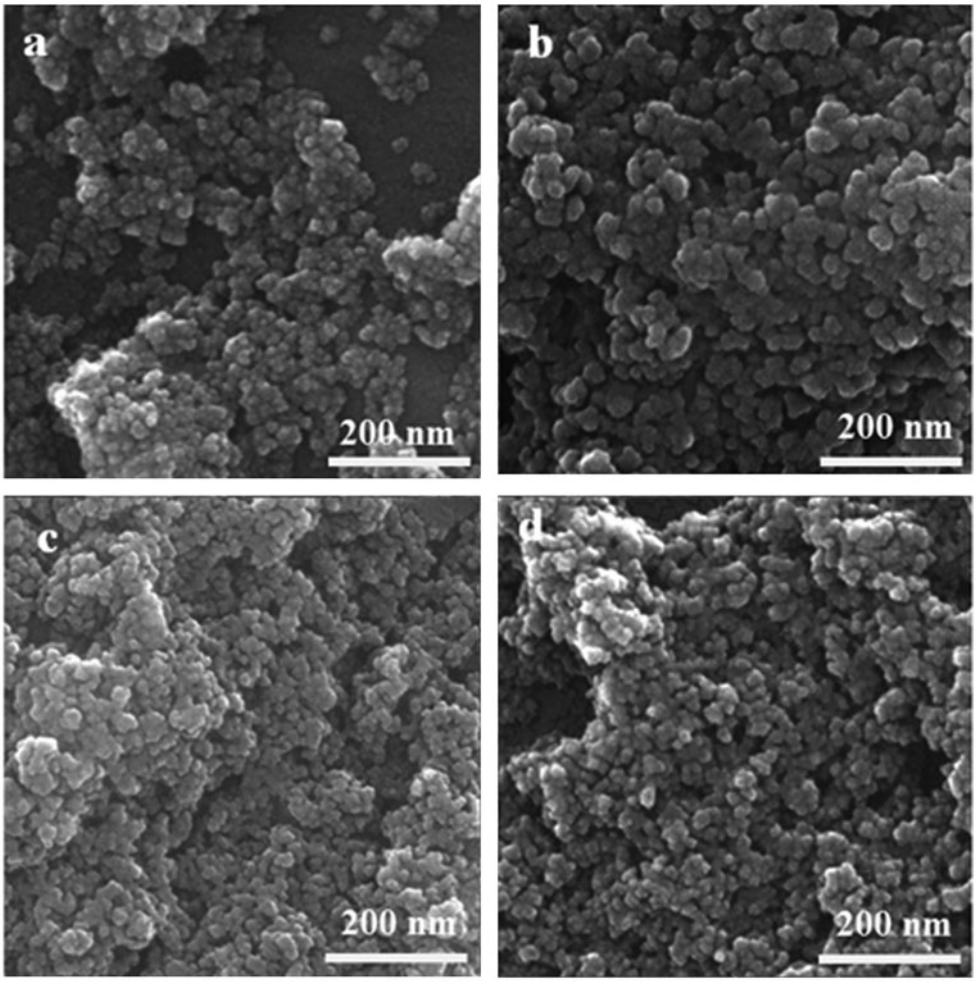

Figure 4. SEM images of (a) Nd–TiO_2 and (b) **1a** (20%); (c) **2a** (20%); (d) **3a** (20%).

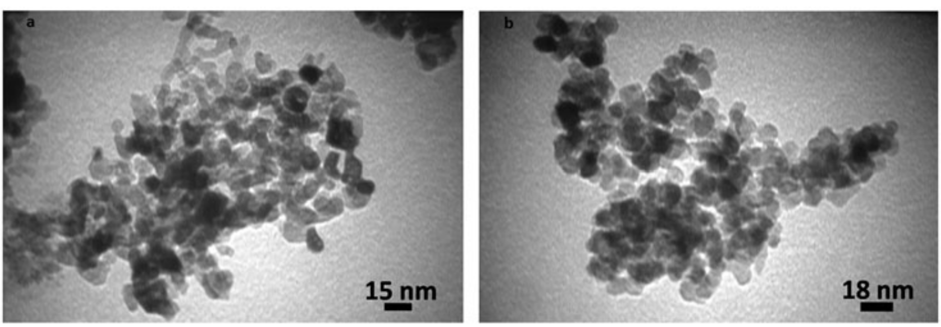

Figure 5. The TEM images of (a) **1a** (20%) and (b) **2a** (20%).

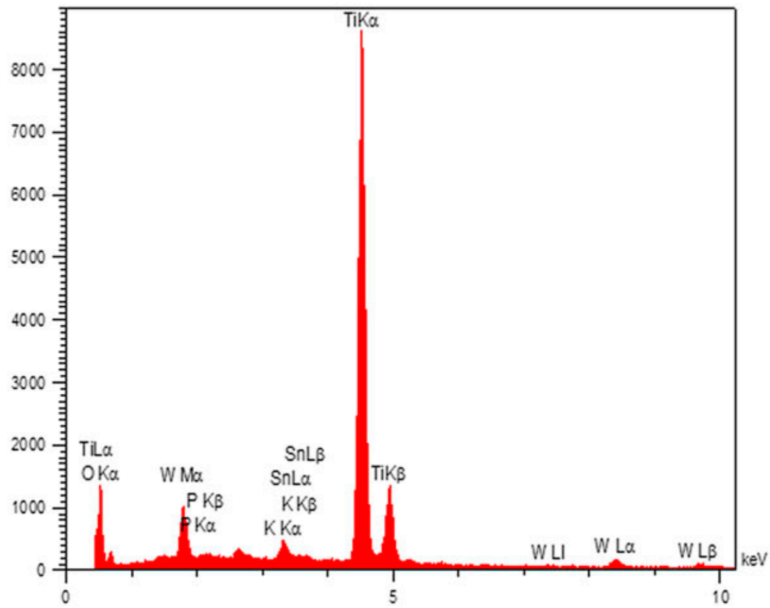

Figure 6. The EDX spectrum of **2a** (20%).

Oxidation of sulfides is the most straightforward method for the synthesis of these valuable materials. Concerning green oxidants, hydrogen peroxide is one of the most powerful candidates next to molecular oxygen because it is inexpensive, readily available, has high atom efficiency, and water is expected to be the only by-product generated from the reaction [48]. Oxidation of sulfides with H_2O_2 is slow; hence, extensive studies have been undertaken to develop new catalysts for this reaction [49–53]. Although these protocols represent considerable progress, there is still a demand for new chemoselective, recoverable and reusable catalysts for the chemoselective oxidation of sulfides to sulfoxide and sulfone using green oxidants. We report the chemoselective oxidation of sulfides to sulfoxides or sulfones with H_2O_2 in the presence of POM–Nd–TiO_2 catalyst. First, in order to find the best catalytic system for the selective oxidation of sulfide, the influence of various catalysts on the oxidation of methyl phenyl sulfide as a model compound using hydrogen peroxide in CH_3CN at room temperature (table 1) was evaluated. As shown in table 1, the reaction was incomplete in the absence of any catalyst and in the presence of catalytic amount of free TiO_2 nanoparticles, Nd–TiO_2 and POMs even after prolonged reaction time (table 1, entries 1–6). All synthesized POM–Nd–TiO_2 (**1a**–**3a**) catalyzed the oxidation of methyl phenyl sulfide to methyl phenyl sulfoxide or sulfone in short reaction times in CH_3CN at room temperature. Catalyst **1a** produced only methyl phenyl sulfoxide while **2a** or **3a** as catalyst led to the corresponding methyl phenyl sulfone under the same reaction conditions (table 1, entries 7–9). To optimize the loading of POMs on Nd–TiO_2 nanoparticles, different loadings of POMs were prepared and used in the oxidation of methyl phenyl sulfide under the same reaction conditions. 20% loading of POMs (50 mg) was found to be ideal for the complete conversion of methyl phenyl sulfide to methyl phenyl sulfoxide or sulfone. When 10% loading of POMs is used, the reactions are completed in the presence of 100 mg of the catalysts (table 1, entries 10-12). The reaction was incomplete in the presence of 40%

loading even after prolonged reaction time (table 1, entry 13). One explanation for reducing the reaction rate is that excess loading (40% and more) probably act as Nd–TiO_2 deactivators. As shown in table 1, with **1a** the reaction is completed in lower time (table 1, entry 10) than nanocomposite containing of **1** loaded on naked TiO_2 nanoparticle, possibly due to synergic effect between TiO_2 and Nd(III) (table 1, entry 14) [54]. When water was used as a solvent instead of CH_3CN, only methyl phenyl sulfoxide was obtained in the presence of catalytic amount of all of three catalysts **1a**–**3a** (table 1, entries 15–17). Therefore, the oxidation of methyl phenyl sulfide to sulfoxide or sulfone in the presence of **2a** or **3a** can be controlled by changing the solvent. To develop the scope of the oxidation of sulfides further, H_2O_2 (6–8 mmol) in the presence of 20% loading of **2a** (50 mg) in H_2O or CH_3CN at room temperature was selected for chemoselective oxidation of sulfides to sulfoxides or sulfones. Various sulfides were subjected to oxidation under the optimized reaction conditions and the expected products were obtained in short times and at high yields (table 2). To show the chemoselectivity of this method, the sulfide containing oxidation-prone functional group (2-thio ethanol) was subjected to oxidation; the OH group remained intact during the conversion of sulfide to sulfoxide or sulfone (table 2, entry 4).

4.1.1. Catalyst recovery and reuse. For practical purposes, recyclability of the catalyst is highly desirable. To investigate this issue, the reusability of **2a** was examined for oxidation of methyl phenyl sulfide as a model substrate. For each of the repeated reactions, the catalyst was easily separated from the product by centrifuge, washed with H_2O and dichloromethane to remove the residual product, dried at 100 °C for 2 h and reused in a subsequent reaction. The catalyst was reused six and 10 times in the oxidation of methyl phenyl sulfide to methyl phenyl sulfoxide and methyl phenyl sulfone, respectively, without a detectable catalyst leaching or a significant loss of its activity (figures 7a and 7b). The FTIR spectrum did not show significant structural changes for catalysts after 10 consecutive runs (figure S6).

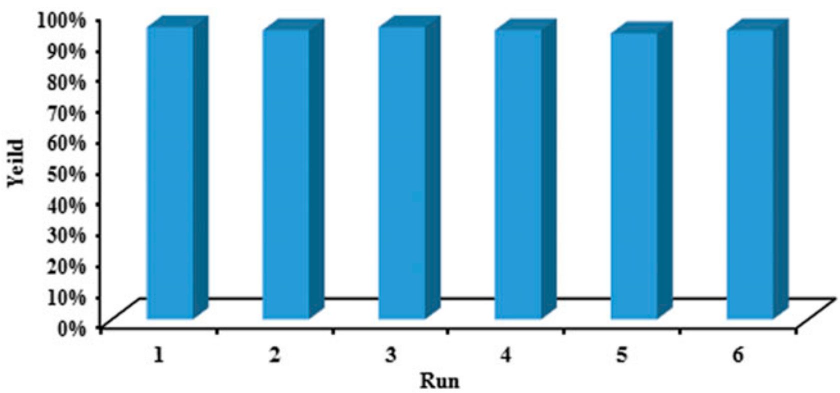

Figure 7a. The recycling experiment of **2a** for the oxidation of methyl phenyl sulfide (1 mmol) to methyl phenyl sulfoxide using H_2O_2 (6 mmol) and in H_2O at room temperature for 5 min.

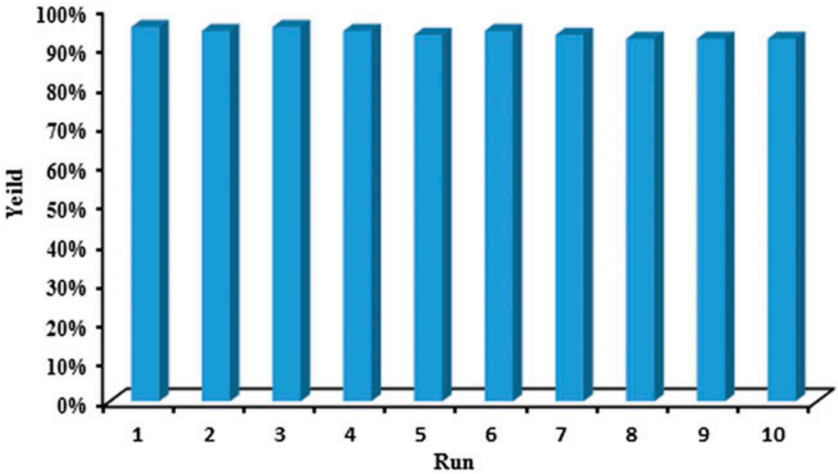

Figure 7b. The recycling experiment of **2a** for the oxidation of methyl phenyl sulfide (1 mmol) to methyl phenyl sulfone using H_2O_2 (6 mmol) and in H_2O at room temperature for 10 min.

4.2. *Catalytic application of POMs–Nd–TiO_2 in the oxidation of benzylic alcohols*

The selective oxidation of alcohols to their corresponding carbonyl compounds is a challenging reaction in organic chemistry [55]. Traditionally, the oxidation of alcohols has been achieved with stoichiometric inorganic oxidants; the disadvantages of these oxidants are that they are expensive, produce large quantities of waste and cause serious environmental problems [56]. Consequently, the use of green and inexpensive oxidants such as oxygen and hydrogen peroxide in effective catalytic systems has attracted attention because of their economic and environmental benefits [57–59]. Owing to the success of POM–Nd–TiO_2 for carrying out oxidation of sulfides, we studied the possibility of applying this new catalyst for the oxidation of alcohols. First, the catalytic activity of various catalysts including Nd–TiO_2, **1**, **2**, **3**, **1a**, **2a,** and **3a** was investigated in the oxidation of benzyl alcohol with 30% hydrogen peroxide as a model reaction in water at 80 °C (table 3). As shown in table 3, in the presence of Nd–TiO_2, **1**, **2,** and **3**, only 10–70% of benzaldehyde was obtained after 24 h (table 3, entries 2–5). When the same reaction was carried out in the presence of **1a**, **2a,** and **3a** (40 mg), benzaldehyde was produced at 100% yield (table 3, entries 6–8). In order to understand more about the activity of these catalysts, oxidations of various alcohols including linear, cyclic, and benzylic ones bearing different functional groups were carried out in water at 80 °C (table 4). The results showed that benzylic alcohols were more reactive than aliphatic substrates and were transformed to the corresponding carbonyl compound with good to high yields. Among benzylic alcohols, electron-rich alcohols are more reactive than electron-poor ones (table 4, entry 2). These results prompted us to explore chemoselectivity of this heterogeneous catalytic system in a binary mixture of benzyl alcohol (as a model for primary benzylic alcohol) and 2-phenyl ethanol (as a model for primary alcohol) in the presence of **2a**. The benzyl alcohol was completely converted to benzaldehyde, while 0% conversion was observed for 2-phenyl ethanol to the corresponding carbonyl compounds (scheme 1).

This reveals that this method can be applied for the chemoselective oxidation of benzylic alcohols in the presence of primary aliphatic alcohols. We have found that **1a** and **2a** in the

Table 4. Selective oxidation of alcohols using H_2O_2 catalyzed by **1a**–**3a** in H_2O.[a]

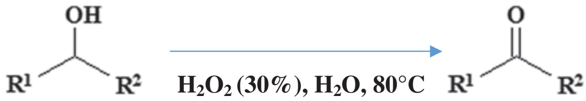

R^1, R^2= H, aryl, benzylic and alkyl

		Time (h)			Isolated yield (%)		
Entry	Substrate	**1a**	**2a**	**3a**	**1a**	**2a**	**3a**
1	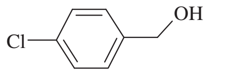	3	3	3	90	90	90
2	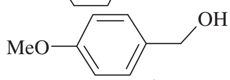	0.5	0.5	1	95	95	95
3	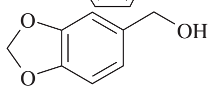	3	3	4	95	95	95
4[b]	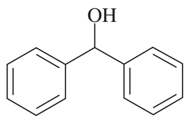	3	3	4	90	90	90
5	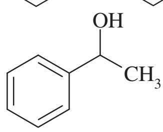	3	3	4	90	90	90
6[c]	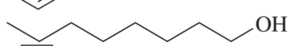	24	24	24	–	–	–
7[c]	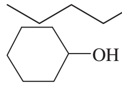	24	24	24	–	–	–
8[c]	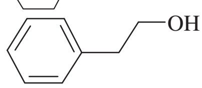	34	34	34	5	5	5

[a]Reaction conditions: alcohol (1 mmol), 30% H_2O_2 (6 mmol), catalysts **1–3a** (40–80 mg), H_2O (1 mL), 80 °C.
[b]PEG was used as solvent.
[c]H_2O_2 (8 mmol), 100 °C.

oxidation of alcohols are more active than **3a**, maybe due to higher charge As(V) and P(V) in the structure of **1a** and **2a** compared to Si(IV) in the structure of **3a**.

4.2.1. Catalyst recovery and reuse. The reusability of the heterogeneous catalyst, **2a**, was examined using benzyl alcohol as a model substrate. After the first use of catalyst in oxidation of benzyl alcohol to give benzaldehyde, the catalyst was easily separated from the product by centrifuge, washed with H_2O and dichloromethane to remove the residual product, dried at 100 °C for 2 h and reused for subsequent experiments under similar reaction conditions. As shown in figure 8, the catalyst was reused at least five times without significant loss of activity.

4.2.2. Reactions mechanism. Catalytic oxidation of various organic substrates with hydrogen peroxide as oxidant may be performed via homolytic or heterolytic cleavage of

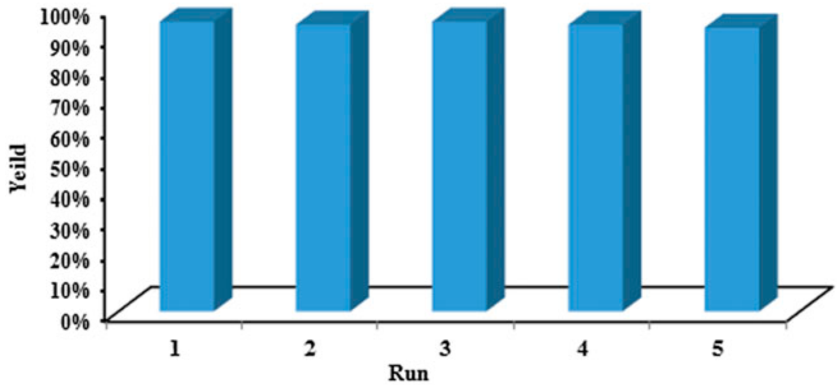

Figure 8. The recycling experiment of **2a** for the oxidation of benzyl alcohol (1 mmol) to benzaldehyde using H_2O_2 (6 mmol) and in H_2O at 80 °C for 3 h.

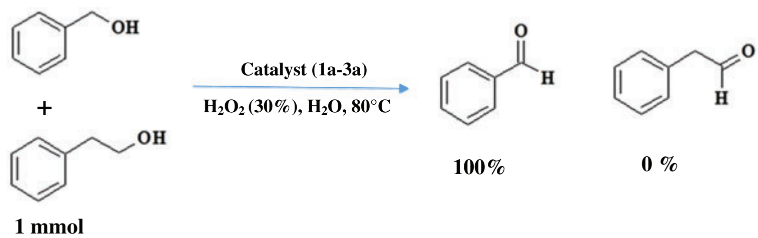

Scheme 1. Chemoselective oxidation of benzyl alcohols in the presence of 2-phenyl ethanol.

the O–O bond. For example, catalytic oxidation of alcohols with inorganic–organic hybrids containing transition metal-substituted polyoxometalates, $[PW_{11}MO_{39}]^{4-}$ for $M = Mn^{2+}$, Fe^{2+}, Co^{2+}, and Cu^{2+}, peroxo-intermediates lead to homolytic cleavage of the O–O bond and produce radicals while, in the case of $M = Zn^{2+}$ the preferred reaction path is heterolytic cleavage of the O–O bond [59]. We ran the oxidation of alcohols and sulfides catalyzed by **1a**, **2a,** or **3a** and hydrogen peroxide as oxidant in the presence of 2,2′-azobis(isobutyronitrile) as radical scavenger. It has been observed that addition of 2,2′-azobis(isobutyronitrile) has no significant effect on the yield of the product or reaction times. This result confirmed that with **1a**, **2a,** or **3a** the preferred reaction path is heterolytic cleavage of the O–O bond.

5. Conclusion

We have developed noncovalently immobilized sandwich-type polyoxometalates $[(HOSn^{IV}OH)_3(XW_9O_{34})_2]^{n-}$ (X = As (**1**), P (**2**) $n = 12$ and Si (**3**) $n = 14$) using Nd–TiO_2 nanoparticles as support. The synthesized catalysts were confirmed by XRD, FTIR, SEM, TEM, and EDX. These catalysts were used for the oxidation of sulfides and benzylic alcohols efficiently in the presence of H_2O_2 (30%) as oxidant. These procedures offer several major advantages,which are as follows: (1) the use of a commercially available, cheap and green oxidant; (2) control over the degree of oxidation it offers sulfoxides or sulfones; (3) excellent chemoselectivity for the oxidation of benzylic alcohols; (4) the heterogeneous catalysts can be easily separated and reused several times; (5) the method conforms to several of the guiding principles of green chemistry.

Disclosure statement

No potential conflict of interest was reported by the authors.

Supplemental data

The PDF file of figures of FTIR of **1**, **1a** (10, 20, 30%) and **3**, **3a** (10, 20, 30%). EDX of **1a** and **3a**. Supplemental data for this article can be accessed http://dx.doi.org/10.1080/00958972.2015.1095889.

References

[1] D.L. Long, E. Burkholder, L. Cronin. *Chem. Soc. Rev.*, **36**, 105 (2007).
[2] M.T. Pope. *Heteropoly and Isopoly Oxometalates*, Springer-Verlag, Berlin (1983).
[3] A. Müller. *Angew. Chem. Int. Ed.*, **43**, 4466 (2004).
[4] I.V. Kozhevnikov. *Chem. Rev.*, **98**, 171 (1998).
[5] C.L. Hill, C.M. Prosser-McCartha. *Coord. Chem. Rev.*, **143**, 407 (1995).
[6] N. Mizuno, M. Misono. *Chem. Rev.*, **98**, 199 (1998).
[7] K. Zhu, D. Wang, J. Liu. *Nano Res.*, **2**, 1 (2009).
[8] X.-M. Yan, J.-H. Lei, D. Liu, Y.-C. Wu, W. Liu. *Mater. Res. Bull.*, **42**, 1905 (2007).
[9] N. Dubey, S.S. Rayalu, N.K. Labhsetwar, S. Devotta. *Int. J. Hydrogen Energ.*, **33**, 5958 (2008).
[10] M.A. Alibeik, Z. Zaghaghi, I.M. Baltork. *J. Chin. Chem.*, **55**, 1 (2008).
[11] R. Neumann, A.M. Khenkin. *J. Mol. Catal. A: Chem.*, **114**, 169 (1996).
[12] R. Neumann, A.M. Khenkin, D. Juwiler, H. Miller, M. Gara. *J. Mol. Catal. A: Chem.*, **17**, 169 (1997).
[13] D. Sloboda-Rozner, P.L. Alsters, R. Neumann. *J. Am. Chem. Soc.*, **125**, 5280 (2003).
[14] (a) C.L. Hill, R.B. Brown. *J. Am. Chem. Soc.*, **108**, 536 (1986); (b) D. Mansuy, J.F. Bartoli, P. Battioni, D.K. Lyon, R.G. Finke. *J. Am. Chem. Soc.*, **113**, 7222 (1991); (c) H. Weiner, Y. Hayashi, R.G. Finke. *Inorg. Chem.*, **38**, 2579 (1999).
[15] X. Zhang, K. Sasaki, C.L. Hill. *J. Am. Chem. Soc.*, **118**, 4809 (1996).
[16] (a) R. Neumann, C. Abu-Gnim. *J. Chem. Soc., Chem. Commun.*, 1324 (1989).(b) R. Neumann, C. Abu-Gnim. *J. Am. Chem. Soc.*, **112**, 6025 (1990).
[17] R. Neumann, A.M. Khenkin. *Chem. Commun.*, 1967 (1998).
[18] (a) R. Ben-Daniel, L. Weiner, R. Neumann. *J. Am. Chem. Soc.*, **124**, 8788 (2002). (b) R. Ben-Daniel, R. Neumann. *Angew. Chem., Int. Ed.*, **42**, 96 (2003).
[19] (a) A.M. Khenkin, R. Neumann. *J. Am. Chem. Soc.*, **124**, 4198 (2002). (b) A.M. Khenkin, R. Neumann. *J. Org. Chem.*, **67**, 7075 (2002).
[20] R. Neumann, M. Dahan. *Nature*, **388**, 353 (1997).
[21] R.A. Sheldon, I.W.C.E. Arends. *Catal. Metal Complexes*, **26**, 123 (2003).
[22] B.S. Lane, K. Burgess. *Chem. Res.*, **103**, 2457 (2003).
[23] M.G. Egusquiza, G.P. Romanelli, C.I. Cabello, I.L. Botto, H.J. Thomas. *Catal. Commun.*, **9**, 45 (2008).
[24] S.S. Balula, M.C. Granadeiro, A.D.S. Barbosa, I.C.M.S. Santos, L. Cunha-Silva. *Catal. Today*, **210**, 142 (2013).
[25] M.R. Farsani, B. Yadollahi, H.A. Rudbari, A. Amini, T. Caradoc-Davis, J.R. Price. *Inorg. Chem. Commun.*, **43**, 39 (2014).
[26] R. Khoshnavazi, L. Bahrami. *J. Coord. Chem.*, **62**, 2067 (2009).
[27] F. Xin, M.T. Pope. *J. Am. Chem. Soc.*, **118**, 7731 (1996).

[28] W.H. Knoth, P.J. Domaille, R.L. Harlow. *Inorg. Chem.*, **25**, 1577 (1986).
[29] W. Yajun, L. Kecheng, F. Changgen. *J. Rare Earths*, **29**, 866 (2011).
[30] V. Stengl, T.M. Grygar. *Int. J. Photoenergy*, **685935**, 1 (2011).
[31] S. Kumar, N.K. Verma, M.L. Singla. *Dig. J. Nanomater. Biostruct.*, **7**, 607 (2012).
[32] P. Periyat, K.V. Baiju, P. Mukundan, P. Krishna Pillai, K.G.K. Warrier. *J. Sol–Gel Sci. Technol.*, **43**, 299 (2007).
[33] F.A. Harraz, O.E. Abdel-Salam, A.A. Mostafa, R.M. Mohamed, M. Hanafy. *J. Alloys Compd.*, **551**, 1 (2013).
[34] Y.X. Zhang, G.H. Li, Y.C. Wu, T. Xie. *Mater. Res. Bull.*, **40**, 1993 (2005).
[35] J. Xu, Y. Ao, M. Chen, D. Fu. *J. Alloys Compd.*, **484**, 73 (2009).
[36] S. Sreekantan, L.C. Wei. *J. Alloys Compd.*, **490**, 436 (2010).
[37] C.E. Zubieta, J.F.A. Soltero-Martinez, C.V. Luengo, P.C. Schulz. *Powder Technol.*, **212**, 410 (2011).
[38] Z. Wang, L. Shi, F. Wu, S. Yuan, Y. Zhao, M. Zhang. *Nanotechnology*, **22**, 1 (2011).
[39] F. Xin, M.T. Pope. *Organometallics*, **13**, 4881 (1994).
[40] W.H. Knoth, P.J. Domaille, R.D. Farlee. *Organometallics*, **4**, 62 (1985).
[41] F. Xin, M.T. Pope, F.J. Long, U. Russo. *Inorg. Chem.*, **35**, 1207 (1996).
[42] M. Yoon, J.A. Chang, Y. Kim, J.R. Choi. *J. Phys. Chem.*, **105**, 2539 (2001).
[43] R.L. McCormick, S.K. Boonrueng, A.M. Herring. *Catal. Today*, **42**, 145 (1998).
[44] H.Y. Zhu, J.A. Orthman, J.Y. Li, J.C. Zhao, G.J. Churchman, E.F. Vansant. *Chem. Mater.*, **14**, 5037 (2002).
[45] Z.L. Shi, F.M. Liu, S.H. Yao. *J. Rare Earths*, **28**, 737 (2010).
[46] Y. Yang, Q.Y. Wu, Y.H. Guo, C.W. Hu, E.B. Wang. *J. Mol. Catal. A: Chem.*, **225**, 203 (2005).
[47] S. Patai, Z. Rappoport. *The Synthesis of Sulfones, Sulfoxides and Cyclic Sulfides*, Wiley, Chichester (1994).
[48] K. Sato, M. Aoki, R. Noyori. *Science*, **281**, 1646 (1998).
[49] K. Sato, M. Hyodo, M. Aoki, X.Q. Zheng, R. Noyori. *Tetrahedron*, **57**, 2469 (2001).
[50] B.M. Choudary, B. Bharathi, C.V. Reddy, M.L.J. Kantam. *J. Chem. Soc., Perkin Trans.*, **1**, 2069 (2002).
[51] M. Kirihara, J. Yamamoto, T. Noguchi, Y. Hirai. *Tetrahedron Lett.*, **50**, 1180 (2009).
[52] A. Rostami, J. Akradi. *Tetrahedron Lett.*, **51**, 3501 (2010).
[53] A. Rostami, B. Atashkar. *J. Mol. Catal., A*, **398**, 170 (2015).
[54] (a) A.K. Pearson, S. Bhargava, V. Bansal. *Langmuir*, **27**, 9245 (2011); (b) E.W. McFarland, H. Metiu. *Chem. Rev.*, **113**, 4391 (2013).
[55] R.A. Sheldon, J.K. Kochi. *Metal-Catalyzed Oxidation of Organic Compounds*, Academic Press, New York (1981).
[56] M. Hudlicky. *Oxidation in Organic Chemistry* (ACS Monograph Series), ACS, Washington (1990).
[57] S. Zhang, G. Zhao, S. Gao, Z. Xi, J. Xu. *J. Mol. Catal. A: Chem.*, **289**, 22 (2008).
[58] Z. Du, H. Miao, H. Ma, Z. Sun, J. Ma, J. Xu. *Adv. Synth. Catal.*, **351**, 558 (2009).
[59] Z. Nadealian, V. Mirkhani, B. Yadollahi, M. Moghadam, S. Tangestaninejad, I. Mohammadpoor-Baltork. *J. Coord. Chem.*, **66**, 1264 (2013).